

# A study on the crystallization speed and thermal stability of N-doped $\text{Ge}_2\text{Sb}_2\text{Te}_5$ thin film during amorphous-to-crystalline phase transition.

KI-HO SONG, JUN-HYONG KIM, JAE-HEE SEO AND HYUN-YONG LEE\*

*Center for Functional Nano Fine Chemicals, Faculty of Applied Chemical Engineering, Chonnam National University, 300 Yongbong-dong, Gwangju 500-757, Korea*

In this work, we evaluated crystallization speed, thermal stability and optical property of the N-doped  $\text{Ge}_2\text{Sb}_2\text{Te}_5$  (GST) thin film, a candidate material for application to a phase-change random access memory (PRAM). The 200-nm-thick GST and N-GST films were deposited on p-type (100) Si and glass substrates using rf reactive sputtering at room temperature. Amorphous-to-crystalline phase transformation of GST and N-GST films was investigated by X-ray diffraction (XRD). The addition of N caused an increase of the crystallization temperature ( $T_c$ ), which means the enhancement of thermal stability for amorphous phase. Changes in the optical transmittance and sheet resistance ( $R_s$ ) of N-GST were observed using an UV-vis-IR spectrophotometer and 4-point probe, respectively. It was found that the added N causes the increase of  $R_s$  for both crystalline and amorphous phases and the optical energy gap ( $E_{OP}$ ). In particular, a high  $R_s$  is useful to reduce programming current. In addition, a speed of amorphous-to-crystalline transition and the surface morphology were evaluated by using a nano-pulse scanner (beam diameter < 2  $\mu\text{m}$ ) and atomic force microscope, respectively. Conclusively, while the N-doping into GST causes the increase of  $T_c$ ,  $R_s$  and  $E_{OP}$ , it accompanies a decrease of crystallization speed.

(Received July 5, 2009; accepted November 12, 2009)

*Keywords:* Crystallization temperature, Amorphous-to-crystalline transition, Phase-change

## 1. Introduction

The demand for non-volatile memories has increased as the market for mobile instruments, such as personal digital assistants (PDA), cellular phone, electronic digital cameras and others has expanded.[1] With its many advantages over other existing memories, a phase change random access memory (PRAM) is considered to be mostly close to a practical utilization and promising candidate as the next generation memory due to many advantages such as high speed, low power, high density, and low cost.[2] The PRAM is based on the reversible phase transformation between amorphous and crystalline states by local heating with a nanosecond current. There have been great efforts on developing new phase-change materials and understanding the phase transformation phenomena in phase-change materials. The pseudo-binary  $\text{Ge}_2\text{Sb}_2\text{Te}_5$  (GST) films have been utilized as a phase-change recording medium.[3] However, there are several problems associated with GST material for high density PRAM devices such as high reset current, thermal stability in amorphous state, relatively.[4] In particular, a high resistance in the crystalline phase is necessary to reduce electrical current.

Thus, nitrogen-doped GST (N-GST) films have been studied with a focus on increasing the electrical resistance of phase change materials.[5] When nitrogen is doped into a GST film, it exists in the forms of nitride or  $\text{N}_2$  molecules, which suppresses crystalline grain growth.[6] However, most studies on the effect of N-doping into

$\text{Ge}_2\text{Sb}_2\text{Te}_5$  film have been concentrated on the macroscopic viewpoint of electrical and optical properties.[7-8] The role of doped nitrogen on the microscopic viewpoint of crystallization speed has not yet been reported.

In this study, we investigated that crystallization speed as well as thermal stability and optical property of N-doped GST in comparison with pseudo-binary GST.

## 2. Experimental details

The 200-nm-thick GST and N-GST films were deposited on p-type (100) Si and glass substrate by rf reactive sputtering at room temperature using  $\text{Ge}_2\text{Sb}_2\text{Te}_5$  composite target. The sputtering was conducted under a power of 50 W, base pressure of  $4 \times 10^{-8}$  Torr and working pressure of  $5 \times 10^{-3}$  Torr. Through the scanning-electron microscope and energy-dispersive X-ray spectroscopy (SEM-EDX) analysis, we confirmed that the composition and thickness of films are under the 5% error range. However we didn't indicate the data in this paper. Nitrogen doping was carried out by adding  $\text{N}_2$  gas into Ar gas within a range of 0-6 sccm for controlling the nitrogen contents in the GST films while the total gas flow rate was fixed at 40 sccm.

Sputtered films were isothermally annealed in a  $\text{N}_2$  atmosphere for 10 min. The isothermal structural phase changes were characterized using X-ray diffraction (XRD, X'pert PRO, Phillips) operated at 40 kV and 40 mA using

Cu K $\alpha$  radiation. XRD measurements were performed for GST and N-GST thin films annealed from 140 °C to 400 °C. The optical transmittance ( $T_{OP}$ ) was measured in the wavelength ( $\lambda$ ) range of 800-3000 nm using a UV-vis-NIR spectrophotometer (Shimadzu, U-3501). The optical absorption coefficient ( $\alpha$ ) was then calculated using the general relation of  $\alpha = -\ln(T_{OP})/d$  and the  $E_{OP}$  was also evaluated using the absorption property expressed as  $\alpha h\nu \propto (h\nu - E_{OP})^2$ . The sheet resistances ( $R_S$ ) of the films were measured with a 4-point probe (CNT-series). The nano-pulse illumination was performed using a nano-pulse scanner with a laser diode of  $\lambda = 650$  nm (beam diameter  $< 2$   $\mu$ m). Speed of the amorphous-to-crystalline phase transition was evaluated by detecting the response reflection signals,  $\Delta R = R_2 - R_1$ , where  $R_1$  and  $R_2$  are the intensities before and after illumination, respectively. In this work,  $\Delta R$  was measured over a laser power ( $P$ ) range of 1 ~ 17 mW and a pulse duration ( $t$ ) range of 10 ~ 460 ns. In addition, the effects of N doping on the surface morphology and roughness of the films were observed by atomic force microscope (AFM).

### 3. Results and discussion

The XRD results for 200-nm-thick GST and N-GST thin films are shown in Fig. 1, where N<sub>2</sub> gas flow rates of

(b), (c) and (d) were approximately 2, 4 and 6 sccm, respectively. As shown in Fig. 1(a), as-deposited and 140 °C-annealed GST thin films did not show any XRD peak, indicating amorphous phase. In general, the Ge<sub>2</sub>Sb<sub>2</sub>Te<sub>5</sub> thin film exhibits two-step crystallization processes. From the Fig. 1(a), the amorphous Ge<sub>2</sub>Sb<sub>2</sub>Te<sub>5</sub> thin film was crystallized into the face-centered-cubic (fcc) structure at about 160 °C. After annealing at 260 °C, the fcc structure was transformed to hexagonal (hcp) structure. However, the structure of N-GST thin films differed from that of GST. In the case of the N (=2, 4 sccm)-doped GST thin films, amorphous phase was maintained up to 200 °C and N (=6 sccm)-doped GST thin film was 260 °C. In addition, when contents of nitrogen increased, crystallized peaks appear to be broader in width and lower in intensity as shown in Fig. 1. Considering that a peak shape of XRD relates to crystalline grain size, the nitrogen doped into GST can be evaluated to serve as a center to suppress crystalline grain growth, resulting in an increase in the crystallization temperature,  $T_C$ , as shown in Fig. 1(b)-(d). [9-10] In particular, the realization of high  $T_C$  leads to an improvement of thermal stability in amorphous state, one of important factors in PRAM devices.

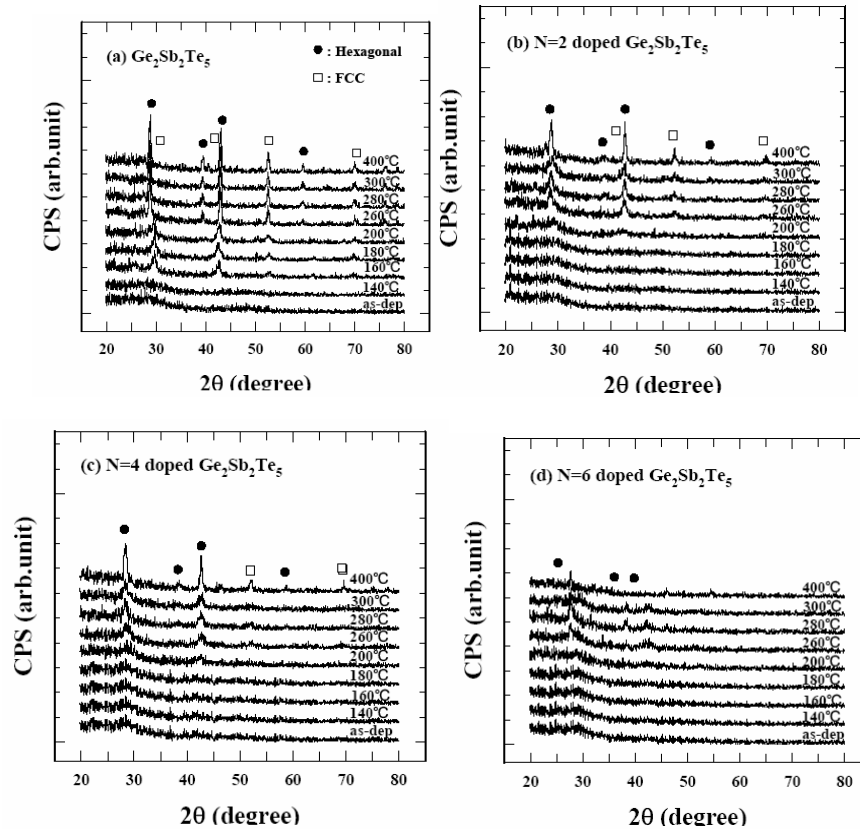


Fig. 1 XRD patterns of 200-nm-thick (a) Ge<sub>2</sub>Sb<sub>2</sub>Te<sub>5</sub>, (b) N= 2 sccm doped, (c) N= 4 sccm doped and (d) N= 6 sccm doped Ge<sub>2</sub>Sb<sub>2</sub>Te<sub>5</sub> thin films as a function of the annealing temperature. The peak marked by the blank (□) and filled (●) correspond to fcc and hcp phases, respectively.

The GST and N-GST thin films were crystallized by annealing at 260 °C for 10 min and their surface morphology observed by AFM was displayed in Fig. 2, where the scale bar on the y-axis of (d) is very large in comparison with those of (a)~(c). As shown in Figs. 2(a) ~ 2(c), the surface morphology appears to be relatively more smooth with increasing N-contents. That is, the crystalline

grain size can be evaluated to decrease with increasing N-contents as discussed in Fig. 1. However, as shown in Fig. 2(d), the hillocks were observed on the surface of N (=6 sccm)-doped GST thin film. It could be considered that these hillocks result from the press of nitrides condensed near grain boundaries.[11]

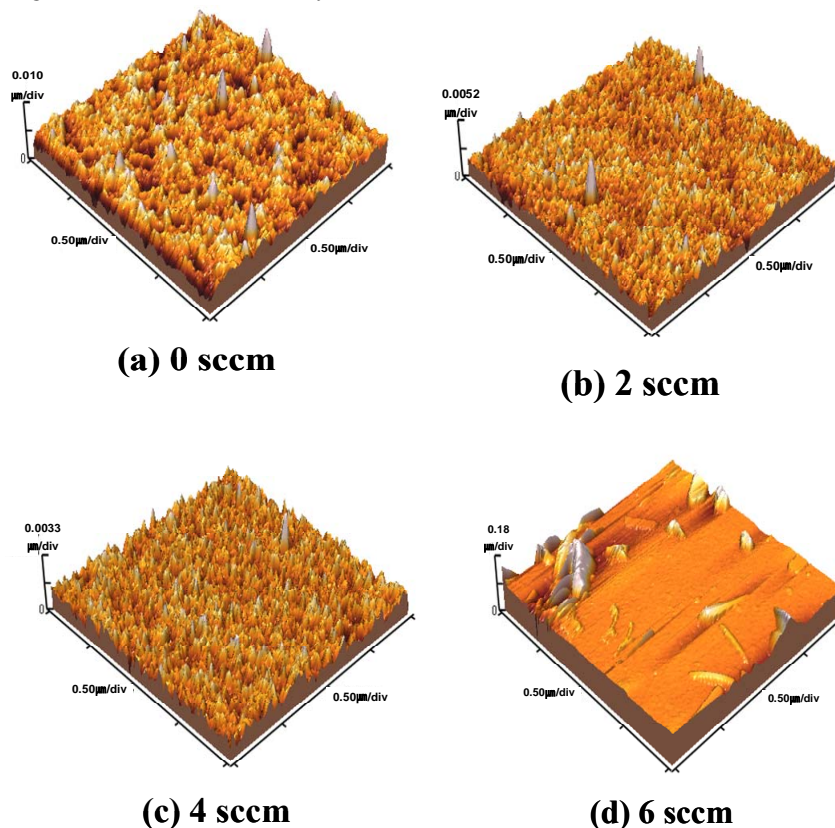


Fig. 2 AFM images of the N-doped  $Ge_2Sb_2Te_5$  thin films annealed at 260 °C for 10 min. The various N contents were (a) 0 sccm, (b) 2 sccm, (c) 4 sccm and (d) 6 sccm. The scale bars on the y-axis is very different; (a) 0.1  $\mu\text{m}/\text{div}$ , (b) 0.0052  $\mu\text{m}/\text{div}$ , (c) 0.0033  $\mu\text{m}/\text{div}$  and (d) 0.18  $\mu\text{m}/\text{div}$ .

The grain size reduction, seen from Figs. 2(b) and 2(c), resulted from the formation of the nitrides like Ge-N, Sb-N and Te-N. [12] This grain size reduction brings about increase of sheet resistance (Fig. 4). Considering that a large change in grain size may deteriorate reliability in the reversible phase-change data storage, N-GST(=2, 4 sccm) film can be evaluated as a candidate material to improve the reliability of PRAM. [4] Quantitative values of surface roughness in the crystallized films (Fig. 2) are shown in Fig. 3 as a function of  $N_2$ -gas flow rate. The roughness slightly decreased with increasing the  $N_2$ -gas flow rate from 0 to 4 sccm but abruptly increased in 6 sccm. That is, a proper N doping (2 and 4 sccm in this work) is effective for smoothing the surface of the crystalline GST film.

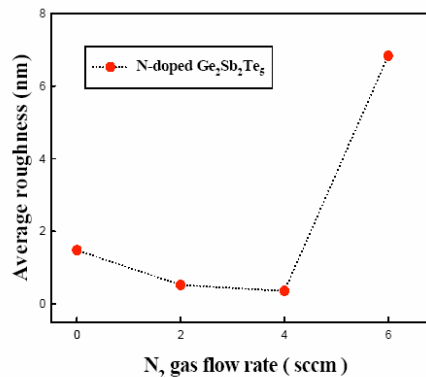


Fig. 3 Average RMS roughness of the N-doped  $Ge_2Sb_2Te_5$  thin films annealed at 260 °C for 10 min.

The temperature-dependent sheet resistance ( $R_S$ ) of phase change material is an important factor. The 4-point probe method was utilized to study the  $R_S$ -dependence of the GST and N-GST films according to annealing temperature and displayed in Fig. 4. The 200-nm-thick GST and N-GST films were annealed in a 200 sccm N<sub>2</sub> atmosphere for 10 min at the temperature ranges of 100 ~ 400 °C, heating rate (dT/dt) ~ 5.0 K/min.

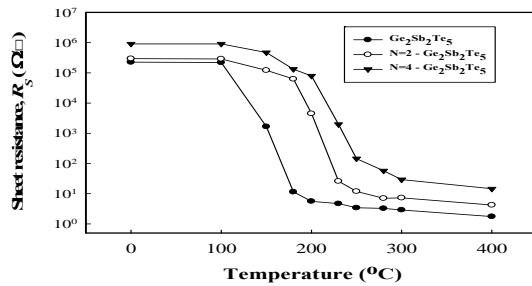


Fig. 4 Changes in sheet resistance ( $R_S$ ) on annealing temperature for the 200-nm-thick Ge<sub>2</sub>Sb<sub>2</sub>Te<sub>5</sub> and N-doped Ge<sub>2</sub>Sb<sub>2</sub>Te<sub>5</sub> films. Films were annealed in a N<sub>2</sub> ambient for 10 min at 100 ~ 400 °C (heating rate ~ 5.0 K/min).

As shown in Fig. 4, the as-deposited GST film (●) of amorphous state showed a high  $R_S$  of  $\sim 10^5 \Omega/\square$ . After annealing at 150 °C, the  $R_S$ -value was drastically reduced to  $\sim 10^1 \Omega/\square$ , which indicates amorphous-to-crystalline (fcc) phase transition. The  $R_S$  of  $10^1 \Omega/\square$  corresponds to the resistivity of  $2 \times 10^{-4} \Omega\text{cm}$ . The incorporation of nitrogen into the GST films increases the  $R_S$  for the overall temperature ranges. In particular,  $R_S$  of the N (=4 sccm) GST films (▼) on the crystalline-phase region (200~400 °C) was higher by one order in comparison with that of GST film. This is related to the grain size reduction by N doping as explained in Fig. 2. The  $R_S$ -dependence on the grain size can be explained as grain boundary scattering mechanism.[13] In addition, although  $R_S$ -values of N-GST were higher than those of the GST, The amorphous/crystalline resistance ratio was constant to be  $\sim 10^5$ . Conclusively, the N-doping causes an increase of  $R_S$  for both amorphous and crystalline phases at all annealed temperatures, which is useful to reduce programming (SET and RESET) current. As shown in Figs. 2 and 4, high  $T_C$ -values obtained by the N doping results in the improvement of thermal stability on the amorphous phase.

Amorphous chalcogenides with a strong electron-lattice interaction obey the absorption properties expressed as  $\alpha h\nu = B(h\nu - E_{OP})^n$  for the extended energy region ( $h\nu > E_{OP}$ ) in which  $B^{1/2}$  is the slope in the extended region ( $h\nu > E_{OP}$ ) and lies in the range  $\sim 10^3 \text{ cm}^{-1/2} \text{ eV}^{-1/2}$  [14-17]. The exponent  $n$  is an appropriately selected index, which depends on the nature of electronic transition and can be assumed to have a value of either 1/2 or 2 for the direct transition and the indirect transition, respectively [18].

Many papers have shown  $n = 2$  acceptable for amorphous chalcogenide semiconductors, including Ge, GeTe, GeSbTe, etc [19-22]. Therefore,  $E_{OP}$  is obtained from the intercept on the energy axis of the plot  $(\alpha h\nu)^{1/2}$  vs.  $h\nu$  as shown in Fig. 5(a). That is,  $E_{OP}$  of GST was evaluated to be  $\sim 0.67 \text{ eV}$ . The quantities of  $E_{OP}$  in the GST and N-GST films were indicated in Fig. 5(b) as a function of the amount of incorporated nitrogen. The incorporation of nitrogen, which mainly formed Ge-N bonds in the GST film [7], increased  $E_{OP}$  in proportion to the amount of N-contents

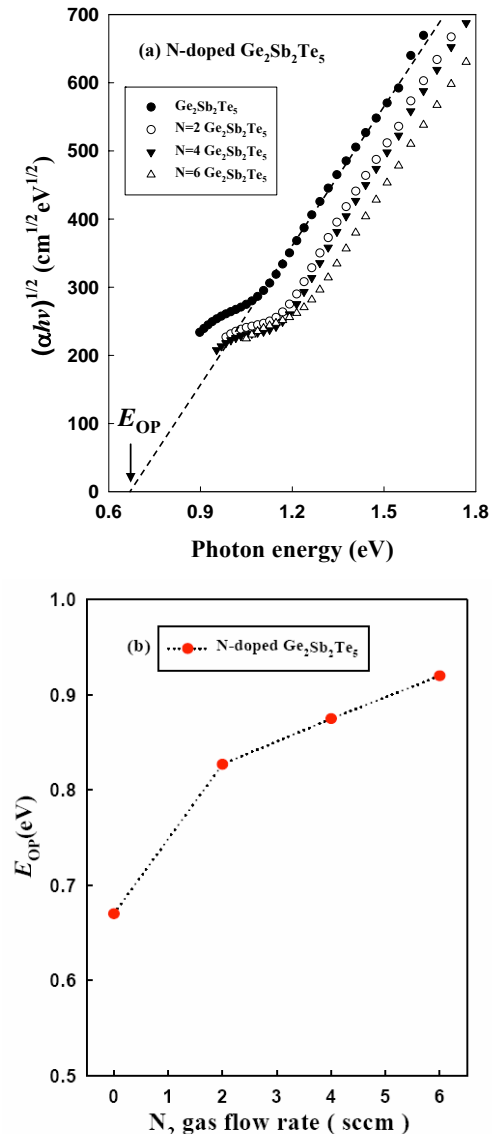


Fig. 5 (a) Plots  $(\alpha h\nu)^{1/2}$  vs.  $h\nu$  for N-doped Ge<sub>2</sub>Sb<sub>2</sub>Te<sub>5</sub> thin films : N=0 sccm(●), N=2 sccm(○), N=4 sccm(▼) and N=6 sccm(△). The optical energy gap ( $E_{OP}$ ) was obtained from the intercept on the energy axis of the plot. (b) Change in  $E_{OP}$  of N-GST films as functions of the amount of incorporated nitrogen.

To investigate the crystallization kinetics on the nanosecond scales, a nano-pulse scanner was employed. The illumination energy by the nano-pulse scanner is systematically controlled as a function of laser power ( $P$ ) and pulse duration ( $t$ ) at each pulse. By this method, the phase transition can be deduced from the changes in

reflectivity. Three-dimensional (3D) mesh plots for the nano-pulse reflection response in the GST and N-GST thin films with increasing  $P$  and  $t$  are shown in Fig. 6, where  $\Delta R$  is the reflection difference ( $R_2 - R_1$ ).

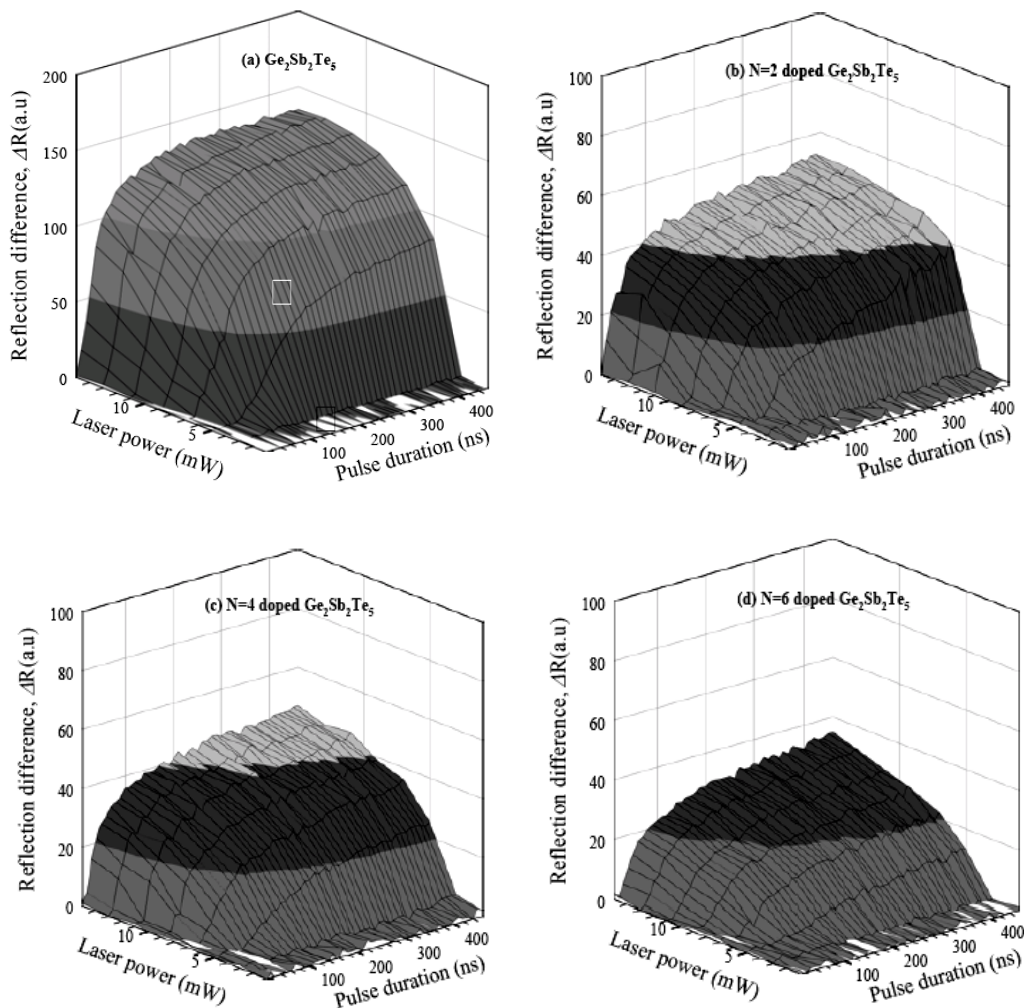


Fig. 6 3D mesh plots for nano-pulse reflection response in the N-SGT ( $N=0, 2, 4, 6$  sccm) thin films. The symbol I and II in (a) represent the amorphous and crystalline regions, respectively. The reflection difference  $\Delta R$  is  $R_1 - R_2$ , where  $R_1$  and  $R_2$  are the intensities before and after illumination, respectively. In this work,  $\Delta R$  was measured in a laser power ranges of 1-17 mW and a pulse duration ranges of 10-460 ns.

The insufficient  $P$  and  $t$  illumination does not generate any change in optical properties (region I). The crystallization (region II) occurs for a proper combination of  $P$  and  $t$ . That is, the  $\Delta R$  value in region I becomes nearly 0 since the power was too low and/or the pulse was

too short to achieve crystallization.  $\Delta R$  in region-II is positive and the film corresponds to a crystalline. As shown Fig. 6, the slopes of  $\Delta R$  vs  $P$  and  $t$  for N-GST films (b, c, d) distinctly decreased compared to that of GST film (a) because the nitride disturbs the crystallization.

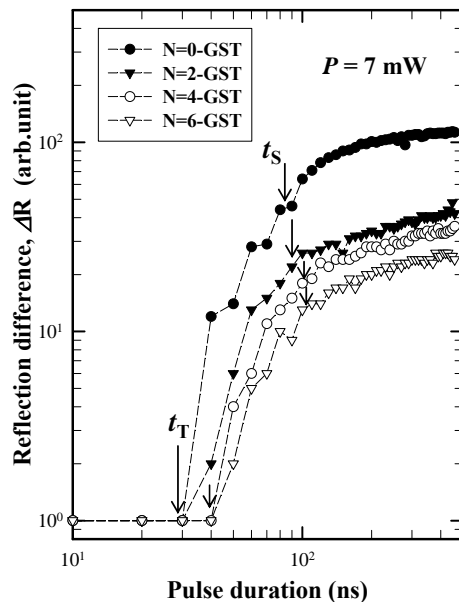


Fig. 7 Log-scaled plot of  $\Delta R$  vs pulse duration ( $t$ ) for a relatively low power (7 mW). The arrows represent the sensitivity  $t_s$  and the threshold pulse duration  $t_T$ .

Figure 7 shows the log-scaled plot of  $\Delta R$  vs  $t$  for a relatively low power (7 mW). Here the arrows represent the sensitivity  $t_s$  defined as a pulse duration corresponding to 50% of the maximum  $\Delta R$ , and  $t_T$  indicates the threshold pulse duration. The nitrogen doping into the GST increased the values of  $t_T$  and  $t_s$  as well as lowered the maximum  $\Delta R$ . For the GST film,  $t_T$  and  $t_s$  were evaluated to be approximately 30 ns and 83 ns, respectively. The  $t_T$  and  $t_s$  values of the N (=4 sccm)-GST film were 40 ns and 98 ns. Therefore, although nitrogen doping into the GST improves the thermal stability on amorphous state and the sheet resistance of both amorphous and crystalline phases, the speed of amorphous-to-crystalline transition is deteriorated.

#### 4. Conclusions

We have investigated influence of nitrogen on the amorphous-crystalline phase transition in the GST thin films. The nitrogen effects can be summarized as follows. According to XRD results, crystallized peaks appear to be broader in width and lower in intensity by doping nitrogen, which shows the crystallization temperature increased. Compared with the GST, N-GST showed higher sheet resistance of both amorphous and crystalline phase because of the grain size reduction. It is useful to reduce programming current. However, the speed of amorphous-to-crystalline transition is relatively very slow by adding nitrogen into the GST. It is considered that the nitrides condense near grain boundaries and have a suppressing effect in the crystallization growth.

In conclusion, although nitrogen doping into GST is a very effective for increasing thermal stability on amorphous state and the sheet resistance of both amorphous and crystalline phases, the speed of amorphous-to-crystalline transition is deteriorated. We propose that the nitrogen into GST plays a role to suppress amorphous-to-crystalline phase transition.

#### Acknowledgments

This work was supported by the Korea Research Foundation (KRF) grant funded by the Korea government (MEST) (No.2009-0064454)

#### Reference

- [1] J. Maimon, E. Spall, R. Quinn and S. Schnur, IEEE Proceedings of Aerospace Conference, Big Sky, MT (IEEE, New York, 2001) p. 2289, (2001)
- [2] Nakayama K, Kitagawa T, Ohmura M, Suzuki M. Jpn. J. Appl. Phys. **32**, 564 (1993)
- [3] Bo. Liu, Zhitang. Song, Ting. Zhang, Jilin. Xia, Songlin. Feng, Bomy. Chen. Thin Solid Films. **478**, 49 (2005)
- [4] Ki. Ho. Song, Sung. Won. Kim, Jae. Hee. Seo, and Hyun. Yong. Lee. J. Appl. Phys. **104**, 103516 (2008)
- [5] Y. K. Kim, U. Hwang, M. H. Cho, Appl. Physics Letters. **90**, 171920 (2007)
- [6] Kihoon. Do, Hyunchul. Sohn, and Dae. Hong. Ko. Journal of The Electrochemical Society. **154**, H867 (2007)
- [7] Y. K. Kim, U. Hwang, Yong. Jai. H. M. Park, and M. H. Cho, Appl. Physics Letters. **90**, 021908 (2007)
- [8] Suk. Min. Kim, Min. Jung. Shin, Doo. Jin. Choi, K. N. Lee, S. K. Hong, Y. J. Park. Thin Solid Films. **469-470**, 323 (2004)
- [9] S. Privitera, E. Rimini, and R. Zonca. Appl. Phys. Lett. **85**, 3044 (2004)
- [10] T. H. Jeong, M. B. Kim, H. Seo, J. W. Park, and C. Yeon. Jpn. J. Appl. Phys., Part 1 **39**, 2775 (2000)
- [11] A. M. Al-Dhafiri, H. A. El-Jammal, A. Al-Shariah, H. A. Naseem, W. D. Brown, Thin Solid Films. **422**, 14 (2002)
- [12] R. Kojjima, S. Okabayashi, T. Kashihara, K. Horai, T. Matsunaga, E. Ohno, N. Yamada, T. Ohta, Jpn. J. Appl. Phys. **37**, 2098 (1998)
- [13] A. K. Kulkarni, Kirk. H. Schulz. T. S. Lim, M. Khan. Thin Solid Films. **345**, 273-277 (1999)
- [14] H. Y. Lee, S.H. Park, J.Y. Chun, and H. B. Chung, J. Appl. Phys. **83**, 5381 (1998)
- [15] K. Tanaka, J. Non-Cryst. Solids. **35-36**, 1023 (1980)
- [16] N. F. Mott and E. A. Davis, Electronic Processes in Non-Crystalline Materials vol 2nd, International Series of Monographs on Physics/Oxford University Press, New York, p. 442 (1979)

- [17] H. Y. Lee, H. B. Chung, *J. Vac. Sci. Technol.* **B 15**, 818 (1997)
- [18] B. Gürbulak, S. Duman, A. Ates, *Czech. J. Phys.* **55**, 93 (2004)
- [19] A. Provano, A. L. Lacaita, A. Benvenuti, F. Pellizzer, R. Bez, *IEEE Trans. Electron Devices.* **51**, 452 (2004)
- [20] B.S Lee, J. R. Abelson, S. G. Bishop, D.H. Kang, B. K. Cheong, K. B. Kim, *J. Apply. Phys.* **97**, 093509 (2005)
- [21] H. Y. Lee, J. W. Kim, H. B. Chung, *J. Non-Cryst. Solids.* **315**, 288 (2003)
- [22] H. Y. Lee, J. Y. Chun, C. H. Yeo, H. B. Chung, *J. Vac. Sci. Technol. A* **18**, 485 (2000)

---

\*Corresponding autho: hyleee@chonnam.ac.kr